*Clay Minerals*, (2018) **53**, 487–496

# Caesium desorption from layer silicate minerals using quaternary ammonium salts

T. MIURA[1,*], A. SASAKI[2], N. SUZUKI[3] AND M. ENDO[1]

[1] *Yamagata University, Graduate School of Science and Engineering, 4-3-16 Jonan, Yonezawa, Yamagata, Japan*
[2] *Yamagata University, Faculty of Engineering, 4-3-16 Jonan, Yonezawa, Yamagata, Japan*
[3] *Showa Pharmaceutical University, 3-3165 Higashi-tamagawa Gakuen, Machida, Tokyo, Japan*

(*Received 12 October 2017; revised 27 May 2018; Guest Associate Editor: M. Elsayed*)

ABSTRACT: The adsorption and desorption of cesium onto layered minerals, zeolite and geochemical reference samples were studied. 0.5 g of bentonite and mica were able to adsorb 71.2 and 51.5 mg of cesium, respectively, from 50 mL of deionized water containing 200 mg/L of cesium under neutral pH condition. These amounts of cesium adsorption were greater than those reported for vermiculites (8.9 and 5.6 mg, respectively). Additionally, the cesium adsorption on mica and vermiculite remained essentially unchanged under seawater conditions, but it decreased drastically on zeolite. The cesium desorption from the layered minerals was promoted by the addition of ammonium ions, namely trioctylmethylammonium chloride and zephiramine. These ammonium ions desorb cesium from the interlayers of the minerals without destroying the mineral structure. The cesium desorption procedure using quaternary ammonium ions would be extremely useful for decontamination of soil containing the layered minerals with adsorbed radioactive cesium.

KEYWORDS: layer silicate minerals, adsorption/desorption of Cs, interlayer swelling, quaternary ammonium salts, seawater, heat treatment.

Inorganic and organic layered minerals are often used as electrode materials, catalysts and adsorbents, among other applications. Layer silicate minerals such as mica, smectite (bentonite) and vermiculite are 2:1-type layer silicates and their structure consists of an alumina sheet sandwiched between two silica sheets (Michael, 2004; Wu *et al.*, 2009; Dzene *et al.*, 2015), as shown in Fig. 1. Positively charged ions are intercalated and adsorbed into the interlayer because the layers are negatively charged (Stagnaro *et al.*, 2012; Abdel-Karim *et al.*, 2016). Smectites are swelling minerals, and their interlayers may swell upon water adsorption to several tens of times their original size (Bostick *et al.*, 2002; Zaunbrecher *et al.*, 2015). The ion-binding forces of cations in minerals follow the sequence $K^+ < Rb^+ \ll Cs^+$ (Sawhney, 1972). Caesium ions move into the interlayers of inorganic layer silicates through ion-exchange reactions, and they are strongly adsorbed without being readily desorbed (Staunton & Roubaud, 1997; Zachara *et al.*, 2002; McKinley *et al.*, 2004; Chiang *et al.*, 2011; Kogure *et al.*, 2012; Kikuchi *et al.*, 2015; Parajuli *et al.*, 2015; Tamura *et al.*, 2015; Mukai *et al.*, 2016). Similar affinity for adsorption of cesium is shown by the zeolites mordenite and clinoptilolite (Endo *et al.*, 2013).

A large amount of Cs was adsorbed onto lamellar minerals in the soil after the accident at Fukushima Daiichi Nuclear Power Plant in 2011 (Murota *et al.*, 2016; Onodera *et al.*, 2017; Mishra *et al.*, 2018). Caesium elution from contaminated materials collected may cause secondary contamination. The adsorption and desorption characteristics of minerals

This paper was originally presented during the session: 'ES-02 Environmental applications of clay minerals' of the International Clay Conference 2017.
*E-mail: t.miura1230@gmail.com
https://doi.org/10.1180/clm.2018.35

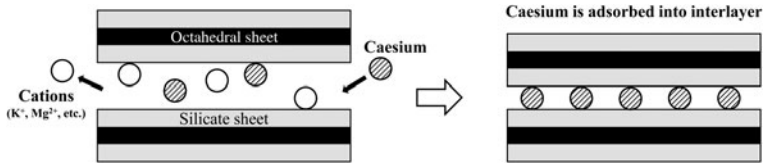


FIG. 1. The structure of a 2:1-type layer silicate mineral displaying Cs adsorption *via* ion exchange.

at the coastline may be influenced by seawater. Therefore, an effective method for inhibiting cesium desorption would be necessary.

In this study, experiments on cesium adsorption and desorption were conducted using various types of layer minerals under various conditions, such as the use of seawater, heat treatment and the presence of cesium desorption agents. The most important objective of this study was to promote cesium desorption. The use of quaternary ammonium salts to expand mineral interlayers and promote cesium desorption was also investigated. Ultimately, a new method for cesium desorption was developed here.

## MATERIALS

An artificial mica (Co-op Chemical Co., Ltd, Japan), a bentonite source of smectite (HOJUN Co. Ltd, Japan), natural vermiculites (CHN: China and ZAF: South Africa), a natural zeolite containing mordenite and clinoptilolite (Itaya, Yamagata, Japan) and geochemical reference samples (basalt JB and soil JSO, AIST) were used in this study. The minerals were ground with a pestle and mortar and sieved through a 0.149 mm sieve. Table 1 lists the five types of quaternary ammonium salts used in desorption tests.

## METHODS

### *Caesium adsorption*

Caesium aqueous solutions with concentrations of 2000 mg/L were prepared by dissolving CsCl powder (Wako Pure Chemical Industries, Ltd, Japan, assay min. 99.0%) in deionized water. 50 mL of 2000 mg/L cesium aqueous solution (amount of Cs added: 100 mg) and 0.5 g of Itaya zeolite, bentonite and mica were placed in a 200 mL polystyrene container and stirred for 2 h (Miura *et al*., 2018). Each solution was filtered through a 0.20 µm syringe filter, and the amount of cesium adsorbed was determined by measuring the cesium concentrations in the filtrates by inductively coupled plasma-mass spectrometry (ICP-MS, ELAN-DRCII, PerkinElmer Japan). In the adsorption experiments with JB and JSO vermiculites, 50 mL of 200 mg/L of cesium aqueous solution was used (amount of Cs added: 10 mg).

Artificial seawater with conductivity of 4.06 S/m and pH 8.39 was prepared from Tetra Marin® Salt Pro (Spectrum Brands Japan Co. Ltd, Japan) with the following composition: Na 8.3 mg/g, Mg 1.2 mg/g, K 0.25 mg/g and Ca 0.43 mg/g. The seawater was adjusted to a predetermined concentration (1.65 g of salt in 50 mL of deionized water). The conductivity of the deionized water was 1.00 mS/m and the pH was 6.68. The experiments for cesium adsorption on minerals in seawater were conducted using the same procedure as that used for cesium adsorption with deionized water. In addition, the layer minerals were calcined in air atmosphere at 400°C, 600°C, 800°C or 1000°C. The cesium adsorption experiments with the calcined minerals were conducted using the same procedure as that used for uncalcined minerals.

The crystal structures were characterized by X-ray diffraction (XRD Ultima IV, Rigaku) using Cu-*K*α radiation, a scanning rate of 10°/min and a scanning step size of 0.02°2θ. The specific surface area of minerals was determined with a surface area analyser (Monosorb Yuasa Ionics Co., Japan) using the Brunauer–Emmett–Teller (BET) equation.

### *Caesium desorption*

Deionized water was used to investigate the desorption behaviour of the minerals examined. The effect of artificial seawater on cesium desorption was also studied. The ratio of mineral and desorption solution was the same as the cesium adsorption test. 25 mL of artificial seawater and 0.25 g of the adsorbent containing cesium were placed in a 200 mL polystyrene container and stirred for 2 h. The solutions were filtered through a 0.20 µm syringe filter. The amount of desorbed cesium was determined from the cesium concentration in each filtrate using ICP-MS. In addition, desorption experiments were performed on minerals saturated with cesium and calcined in air at

https://doi.org/10.1180/clm.2018.35 Published online by Cambridge University Press

TABLE 1. Quaternary ammonium salts used for cesium-desorption tests.

| Quaternary ammonium salt | Chemical formula | Structural formula |
|---|---|---|
| DTMAC (dodecyltrimethylammonium chloride) | $C_{15}H_{34}ClN$ | 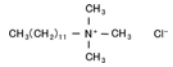 |
| TTDAC (trimethyltetradecylammonium chloride) | $C_{17}H_{38}ClN$ | 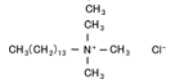 |
| TDTAB (tetradecyltrimethylammonium bromide) | $C_{17}H_{38}BrN$ | 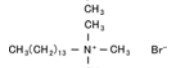 |
| TOMAC (trioctylmethylammonium chloride) | $(R_3NCH_3)Cl$ | 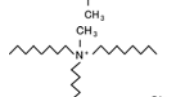 |
| Zephiramine | $C_{23}H_{42}ClN{\cdot}2H_2O$ | 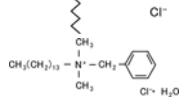 |

400°C, 600°C, 800°C or 1000°C using hydrochloric acid (Matsumoto, 2002; Miura *et al.*, 2018). The cesium desorption experiments for the calcined minerals with 0.1 mol/L hydrochloric acid were conducted using the same procedure as that used for cesium desorption without calcination.

The surface morphologies of the calcined minerals were determined using scanning electron microscopy (SEM; JSM-7600FA, JEOL).

### *Caesium desorption using quaternary ammonium salts*

Before cesium desorption tests, adsorption tests on layer minerals were performed in the presence of quaternary ammonium salts to evaluate their effects on the interlayer expansion. Straight-chain quaternary ammonium salts (dodecyltrimethylammonium chloride [DTMAC], trimethyltetradecylammonium chloride [TTDAC] and tetradecyltrimethylammonium bromide [TDTAB]) and non-straight-chain quaternary ammonium salts (trioctylmethylammonium chloride [TOMAC] and zephiramine) were used in the tests. The concentration of the ammonium solutions was prepared according to all ammonium reagents that may be dissolved in deionized water. Each ammonium solution (50 mL, 0.01 mol/L) and a mineral sample (0.5 g) were placed in a 200 mL polystyrene container and were stirred for 2 h. The mineral was filtered using filter paper and dried at room temperature. The interlayer distances of the minerals were obtained from the XRD peaks.

The ratio of mineral to desorption solution was the same as the cesium adsorption test. The desorption solution, comprising 25 mL of each of 0.01 mol/L ammonium solution, and 0.25 g of minerals with adsorbed cesium were placed in a 200 mL polystyrene container and stirred for 2 h. The solutions were filtered through a 0.20 μm syringe filter. The amount of desorbed cesium was determined in each filtrate with ICP-MS.

TABLE 2. $q_{max}$ saturated amounts of cesium adsorbed onto all minerals in deionized water or seawater.

| | Deionized water (mg) | Seawater (mg) |
|---|---|---|
| Itaya zeolite | 104.1 | 8.3 |
| Bentonite | 71.2 | 18.8 |
| Mica | 51.5 | 60.0 |
| Vermiculite (CHN) | 8.9 | 8.3 |
| Vermiculite (ZAF) | 5.6 | 1.5 |
| JB | 2.6 | 0.8 |
| JSO | 1.9 | 0.9 |

## RESULTS AND DISCUSSION

### *Caesium adsorption characteristics*

Caesium ions are adsorbed within the interlayer of layer silicates and in the channels of zeolites through ion exchange (Benedicto *et al.*, 2014). The amount of cesium adsorbed on Itaya zeolite (104.1 mg) was greater than that on the layer minerals and geochemical

https://doi.org/10.1180/clm.2018.35 Published online by Cambridge University Press

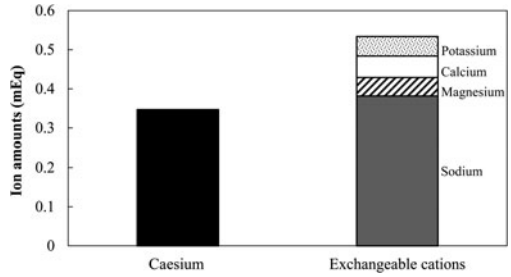


FIG. 2. Eluted amounts (mEq) of cations from mica during cesium adsorption.

reference samples for each initial concentration (Table 2). In addition, the amounts of cesium adsorbed on mica and bentonite (51.5 and 71.2 mg) were greater than those on vermiculites (CHN: 8.9 mg and ZAF: 5.6 mg), meaning that the mica and bentonite were saturated with cesium. Montmorillonite swells infinitely in water and may adsorb large amounts of cesium (Onikata *et al.*, 1999; Bostick *et al.*, 2002; Zaunbrecher *et al.*, 2015). Therefore, large amounts of cesium were adsorbed on mica, bentonite and Itaya zeolite because of the water-swelling ability of smectite in bentonite and the large numbers of exchangeable cations in the zeolite channels and the large interlayer occupancy in mica.

Smectites in bentonite are water-swelling minerals and, in water, their interlayer distance increases to several tens of times its original size. Vermiculites are lamellar minerals with the same structure as mica and smectite. However, the amount of cesium adsorbed on vermiculite was less than that on bentonite. These results suggest that an increase in the interlayer space due to water swelling promotes the intercalation of cesium ions. In micas, adsorption of cesium may be linked to the frayed-edge wedged surfaces (Zachara *et al.*, 2002; Zaunbrecher *et al.*, 2015). Because the adsorption of cesium and strontium on montmorillonite and zeolites has been observed to follow the Langmuir-type isotherm (Mimura & Kanno, 1985; Wu *et al.*, 2009), it was assumed that the cesium adsorption in this study also followed the Langmuir model. The $q_{max}$ saturated adsorption amounts of cesium are listed in Table 2.

The major exchangeable cations in the minerals studied are Na, Ca, Mg and K. Figure 2 shows the result of eluting exchangeable cations during cesium adsorption. The exchangeable cations varied for different types of minerals. Mainly Na ions were eluted from mica and smectite (bentonite) during cesium adsorption, suggesting that these minerals were Na-rich. On the other hand, cesium adsorption on Itaya zeolite was followed by the release of Na, Ca and K ions. In vermiculite, JB and JSO, the exchangeable cations were mainly Ca and Mg. The specific surface area of zeolite (95.6 $m^2/g$) was larger than other minerals (bentonite: 25.3 $m^2/g$, mica: 31.7 $m^2/g$, CHN vermiculite: 9.3 $m^2/g$, ZAF vermiculite: 6.3 $m^2/g$, JB: 5.7 $m^2/g$ and JSO: 9.3 $m^2/g$). The amounts of cesium adsorbed on the minerals varied in accordance with the specific surface area.

Table 2 also lists the experimental results of cesium adsorption on minerals in artificial seawater. The amounts of cesium adsorbed in seawater for all minerals except mica were less than those in deionized water. The amounts of cesium adsorbed in seawater with respect to distilled water for Itaya zeolite, bentonite, mica, vermiculite (CHN), vermiculite (ZAF), JB and JSO were 8.0 (8.3 mg/104 mg × 100 = 8.0%), 26.4, 116.5, 93.3, 26.8, 30.8 and 47.4%, respectively. The main component of the artificial seawater is sodium (8.3 mg/g). The selective adsorption of cations on minerals follows the sequence $Mg^{2+} < Ca^{2+} < Na^{+} < K^{+} < NH_4^{+} < Cs^{+}$ (Sawhney, 1972; Staunton & Roubaud, 1997). The adsorption of cesium

TABLE 3. Caesium adsorption and desorption ratios (wt.%) of calcined minerals at various calcination temperatures relative to the cesium adsorption amounts of the respective minerals in Table 2 before calcination in deionized water.

| | Adsorption ratio of cesium (wt.%) | | | | Desorption ratio of cesium (wt.%) | | | |
|---|---|---|---|---|---|---|---|---|
| | 400°C | 600°C | 800°C | 1000°C | 400°C | 600°C | 800°C | 1000°C |
| Bentonite | 66 | 49 | 32 | 20 | 22.6 | 23.2 | 17.2 | 0.5 |
| Mica | 89 | 89 | 89 | 39 | 2.6 | 3.1 | 1.8 | 1.6 |
| Vermiculite (CHN) | 67 | 29 | 14 | 11 | 0.8 | 1.8 | 1.5 | 0.8 |
| Vermiculite (ZAF) | 100 | 73 | 21 | 7 | 15.5 | 9.4 | 4.0 | 2.2 |

https://doi.org/10.1180/clm.2018.35 Published online by Cambridge University Press

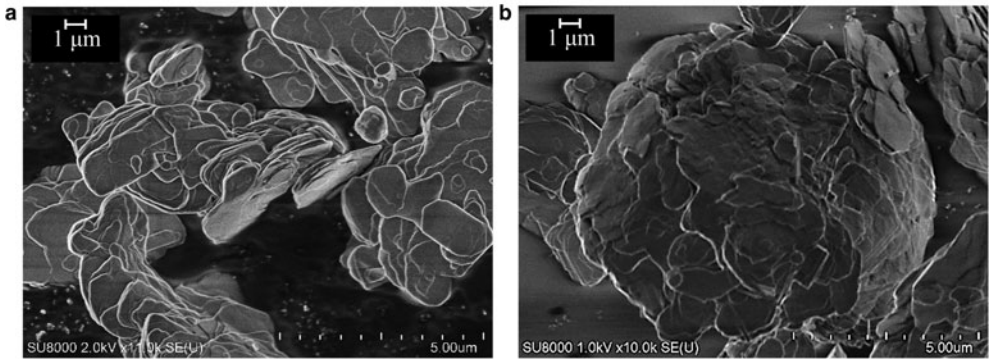


FIG. 3. SEM images of mica (a) before calcination and (b) after calcination at 1000°C.

was affected mainly by the abundance of Na ions in the artificial seawater rather than other ions such as Mg. The coexistence of other cations in artificial seawater decreased the adsorption rate of cesium on the various minerals except for mica. Previous work has shown that mica selectively adsorbs Cs ions (Sawhney, 1972; Zachara *et al.*, 2002), which are fixed rigidly in frayed interlayer sites and are rarely displaced (McKinley *et al.*, 2004; Kogure *et al.*, 2012; Kikuchi *et al.*, 2015). Therefore, the large amount of cesium in seawater was adsorbed onto mica.

The amount of cesium adsorbed on mica in seawater (60.0 mg) was greater than that in deionized water (51.5 mg), suggesting that the adsorption properties of mica were not influenced by the Na, K, Ca and Mg ions. As the mica and seawater used in this study are artificial materials without corrosion products, the cesium-adsorption characteristics of mica in this study were not influenced by corrosion. However, the presence of humic acids has been reported to enhance cation adsorption on minerals (Komy *et al.*, 2014). It is considered, therefore, that the coexistence of corrosion products would be influenced by the cesium-adsorption characteristic in a real, natural environment.

The main component of natural bentonite is montmorillonite. Electrolyte solutions such as seawater suppress Na-montmorillonite swelling (Onikata *et al.*, 1999). Hence, cesium adsorption on bentonite was strongly influenced by seawater in this study. In contrast, the mica used in this study was not affected thus and is expected to be applied successfully as a cesium adsorbent in the presence of seawater. In addition, the influence of the seawater on the adsorption behaviour of vermiculite (CHN) was low compared with that of vermiculite (ZAF), suggesting that origin affects the cesium adsorption characteristics of minerals.

The cesium adsorption ratios of the calcined minerals decreased with increasing calcination temperature (Table 3). Figure 3 shows SEM images of the mica's surface before and after calcination at 1000°C. The surface became smooth after calcination at 1000°C, indicating softening and possible melting, and similar observations were made for the remaining minerals. This morphological change in the mineral surface affects the cesium-adsorption characteristics, as the cesium adsorption ratio reached a minimum value at 1000°C for all minerals. Melting of the mineral surface and trapped exchangeable cations at ion-exchange sites in the minerals hindered cesium adsorption.

TABLE 4. Caesium-desorption ratios (wt.%) of minerals (0.25 g) in deionized water or seawater relative to the amounts of Cs adsorbed by the minerals (Table 2).

| | Deionized water | Seawater |
|---|---|---|
| Bentonite | 3.9 | 37.2 |
| Mica | 1.5 | 10.8 |
| Vermiculite (CHN) | 0.2 | 6.4 |
| Vermiculite (ZAF) | 1.5 | 31.5 |

### *Caesium-desorption characteristics*

The ion-exchange reactions of minerals in aqueous solution affect the desorption behaviour of cesium. The ion-exchange reaction during cesium desorption with deionized water is between cesium ions and protons. The cesium-desorption ratios of vermiculites were

https://doi.org/10.1180/clm.2018.35 Published online by Cambridge University Press

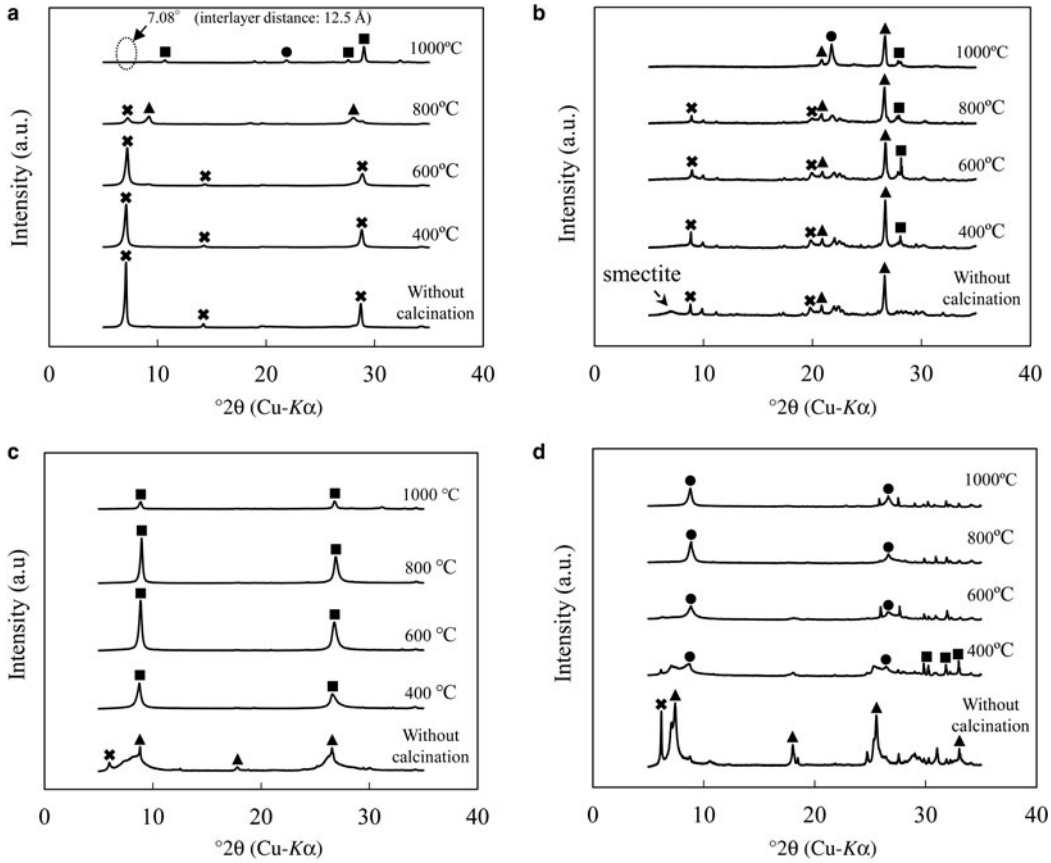


FIG. 4. XRD patterns of: (a) mica, (b) bentonite, (c) vermiculite (CHN) and (d) vermiculite (ZAF) calcined at various temperatures (Cu-*K*α, scan rate: 10°2θ/min and step scan size 0.02°2θ). (a) ×, ▲: collapsed mica; ■: fluor-magnesio-arfvedsonite; ●: cristobalite; (b) ×: mica (illite); ▲: quartz; ■: albite; ●: cristobalite. (c) ×: vermiculite; ▲: phlogopite; ■: phlogopite; (d) ×: vermiculite; ▲: hydrobiotite; ■: diopside; ●: phlogopite.

greater than those of mica and bentonite (Table 4). Combining the results in Tables 2 and 4, the cesium-desorption ratio increased inversely with the amount of cesium adsorbed on the minerals. The amounts of cesium desorbed from mica and bentonite were small, suggesting that these minerals have a high affinity for Cs ions.

The cesium desorption ratios of mica and vermiculite (CHN) in seawater were less than those of bentonite and vermiculite (ZAF) (Table 4). The cesium desorption ratios of mica and bentonite were 10.8 wt.% (112 ppm) and 37.2 wt.% (530 ppm), respectively. Therefore, cesium desorption from mica was barely affected by seawater, as was also the case for its adsorption. The cesium adsorbed onto mica was barely desorbed from the frayed interlayer because of the control of the mica layer structure on cesium retention (Delvaux *et al.*, 2000; Nakao *et al.*, 2014). Mica is an abundant lamellar mineral at Fukushima in Japan that selectively adsorbs cesium (Mukai *et al.*, 2016). In this study, it was confirmed that Cs ions were adsorbed readily onto and barely desorbed from mica in seawater. Therefore, developing new methods of cesium desorption from the lamellar minerals was critical. The cesium-desorption ratio of vermiculite (CHN) was also small due to the minimal effect of seawater.

The desorption ratios of cesium for all minerals decreased with increasing calcination temperature to 1000°C, similar to cesium adsorption on calcined minerals (Table 3). The observed decrease in cesium is due to melting of the mineral surface and trapping of

https://doi.org/10.1180/clm.2018.35 Published online by Cambridge University Press

TABLE 5. The interlayer distances (Å) of bentonite, mica and vermiculite. The quaternary ammonium salts were adsorbed on these minerals. Bold numbers indicate expanded interlayer distances.

| | Mica ME-100 | Bentonite | Vermiculite (CHN) |
|---|---|---|---|
| Literature value | 12.2 | 9.6 | 14.0 |
| Value measured in the present study before treatment | 12.5 | 10.0 | 14.8 |
| $Cs^+$ adsorbed | 10.7 | 10.0 | 10.5 |
| DTMAC | **18.2** | **11.1** | **15.2** |
| TTDAC | **13.8** | 10.0 | 10.1 |
| TDTAB | **14.8** | **10.7** | 14 |
| TOMAC | 10.8 | 10.1 | 14.2 |
| Zephiramine | **13.1** | 10.0 | 10.1 |

cesium. The XRD patterns of layer silicates before and after calcination are shown in Fig. 4. The clear peak at 7.08°2θ (12.5 Å interlayer distance) in the XRD pattern of mica before calcination disappeared after calcination at 1000°C (Fig. 4a), and the XRD peak intensities decreased as the calcination temperature increased, suggesting that the structures of all minerals collapsed during heating. The structural modifications of the minerals were observed in the XRD patterns. The layer structure collapsed and the interlayer distance decreased during heating.

### *Characteristics of cesium desorption induced by quaternary ammonium salts*

Intercalation of organic compounds may induce peeling and expanding of the interlayers in layer silicates (Onikata *et al.*, 1999; Royer *et al.*, 2010). The effects of quaternary ammonium salts on interlayer expansion in mica, bentonite and vermiculite (CHN) were investigated.

Table 5 shows the literature values of interlayer distances for layered minerals (Kahr *et al.*, 1986; Peeterbroeck *et al.*, 2005; Dzene *et al.*, 2017), which are in accord with the interlayer spaces recorded in this experiment. The quaternary ammonium salt would intercalate into the interlayer of the lamellar mineral due to electrostatic attraction replacing interlayer cations. The straight-chain quaternary ammonium salts (DTMAC, TTDAC and TDTAB) increased the interlayer distance of the minerals, as recorded by XRD. On the other hand, the branched quaternary ammonium salts (TOMAC and zephiramine) did not intercalate in the interlayer spaces of minerals. It was

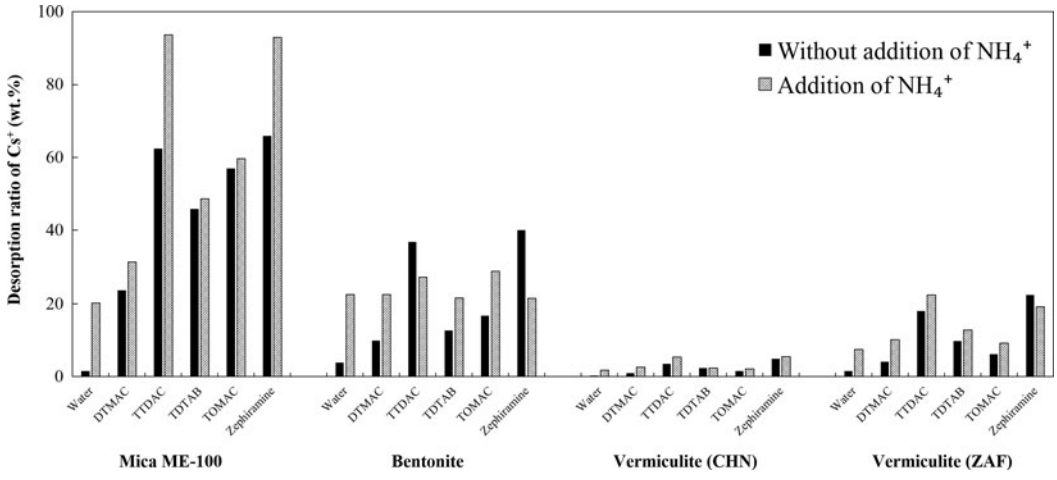


FIG. 5. Caesium-desorption ratios (wt.%) of mica, bentonite and vermiculites (0.25 g) using quaternary ammonium salts (0.01 mol/L, 25 mL) relative to the amount of cesium adsorbed on bentonite (Table 2).

https://doi.org/10.1180/clm.2018.35 Published online by Cambridge University Press

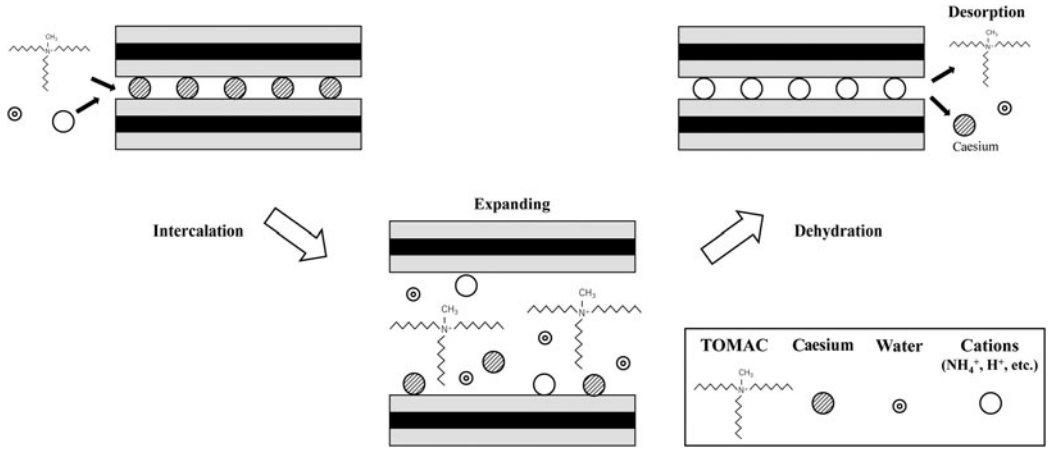


FIG. 6. A schematic diagram showing the characteristics of cesium desorption from a water-swelling mineral using TOMAC.

suggested that the branched quaternary ammonium salts desorbed from the interlayers together with dehydration of the interlayer.

Caesium ions scarcely desorbed from the lamellar minerals during cesium-desorption tests. However, the cesium desorption ratios increased upon intercalation of quaternary ammonium salts (Fig. 5). Caesium desorption was promoted by the addition of ammonium ions to the desorption solution; this is because the ionic radius of ammonium is similar to that of cesium. The ratios of cesium desorbed from minerals after reaction with TTDAC and zephiramine were greater than those after reaction with other quaternary ammonium salts. In addition, desorption of cesium ions was more pronounced when straight-chain quaternary ammonium salts with longer chains were used because longer straight-chain quaternary ammonium salts may expand over a wider area of the interlayer. Chloride was more suitable than bromide as the counter ion of quaternary ammonium salts for cesium desorption. The amounts of cesium desorbed from vermiculites were small with TOMAC, which has three alkyl chains, and zephiramine, which has one benzene ring; this is probably because TOMAC and zephiramine were not intercalated into the interlayers of vermiculites. On the other hand, vermiculites would only be intercalated by straight-chain quaternary ammonium salts with a small molecular size because of the small induced expansion of the vermiculite interlayer. Therefore, the selection of quaternary ammonium salts for cesium desorption depends on the swelling capacity of the layer mineral.

Furthermore, the interlayer distances of minerals (Table 5) and the desorption experiment results with quaternary ammonium salts (Fig. 5) were compared. According to the XRD results, the straight-chain quaternary ammonium salts were adsorbed into the mineral interlayers, causing swelling. Nevertheless, the desorption ratios of cesium were promoted by the branched quaternary ammonium salts. These results were influenced by the water content of the mineral. Therefore, expansion of the mineral interlayer distance in Table 5 was not confirmed because TOMAC and zephiramine were desorbed from the interlayer together with dehydration. In addition, cesium was desorbed from the mineral interlayer together with the desorption of TOMAC and zephiramine (Fig. 6). Although cesium was desorbed from the mineral interlayer, the structure was not affected by desorption.

## CONCLUSIONS

The amounts of cesium adsorbed on hydrated mica and bentonite were greater than those on vermiculites because of the water-swelling ability of smectite interlayers or the large numbers of exchangeable cations at mica adsorption sites. The exchangeable cations relevant to cesium adsorption varied for different minerals. Caesium desorption in deionized water was affected by the affinity of Cs ions for the mineral. Caesium adsorption and desorption for minerals other than mica and vermiculite (CHN) in seawater were less and greater, respectively, than in

https://doi.org/10.1180/clm.2018.35 Published online by Cambridge University Press

deionized water. It was confirmed that the cesium adsorption and desorption characteristics of mica and vermiculite (CHN) were barely affected by seawater. The cesium adsorption and desorption ratios of the calcined minerals decreased with increasing calcination temperature due to softening and possibly melting of the minerals and trapping of cesium. A particularly important finding of the present study is that TOMAC and zephiramine may be used to desorb cesium from mineral interlayers without affecting the structure of the mineral.

## REFERENCES


Abdel-Karim A.M., Zaki A.A., Elwan W., El-Naggar M.R. & Gouda M.M. (2016) Experimental and modeling investigations of cesium and strontium adsorption onto clay of radioactive waste disposal. *Applied Clay Science*, **132–133**, 391–401.

Benedicto A., Missana T. & Fernández A.M. (2014) Interlayer collapse affects on cesium adsorption onto illite. *Environmental Science & Technology*, **48**, 4909–4915.

Bostick B.C., Vairavamurthy M.A., Karthikeyan K.G. & Chorover J. (2002) Caesium adsorption on clay minerals: an EXAFS spectroscopic investigation. *Environmental Science & Technology*, **36**, 2670–2676.

Chiang P.N., Wang M.K., Huang P.M. & Wang J.J. (2011) Effects of low molecular weight organic acids on $^{137}$Cs release from contaminated soils. *Applied Radiation and Isotopes*, **69**, 844–851.

Delvaux B., Kruyts N. & Cremers A. (2000) Rhizospheric mobilization of radiocesium in soils. *Environmental Science & Technology*, **34**, 1489–1493.

Dzene L., Ferrage E., Viennet J.C., Tertre E. & Hubert F. (2017) Crystal structure control of aluminized clay minerals on the mobility of caesium in contaminated soil environments. *Scientific Report*, **7**, 43187.

Dzene L., Tertre E., Hubert F. & Ferrage E. (2015) Nature of the sites involved in the process of cesium desorption from vermiculite. *Journal of Colloid and Interface Science*, **455**, 254–260.

Endo M., Yoshikawa E., Muramatsu N., Takizawa N., Kawai T., Unuma H., Sasaki A., Masano A., Takeyama Y. & Kahara T. (2013) The removal of cesium ion with natural Itaya zeolite and the ion exchange characteristics. *Journal of Chemical Technology & Biotechnology*, **88**, 1597–1602.

Kahr G., Kraehenbuehl F., Müller-Vonmoos M. & Stoeckli H.F. (1986) *Wasseraufnahmeund Wasserbewegung in Hochverdichtetem Bentonit*. Nagra, Baden, Switzerland.

Kikuchi R., Mukai H., Kuramata C. & Kogure T. (2015) Cs-sorption in weathered biotite from Fukushima granitic soil. *Journal of Mineralogical and Petrological Sciences*, **110**, 126–134.

Kogure T., Morimoto K., Tamura K., Sato H. & Yamagishi A. (2012) XRD and HRTEM evidence for fixation of cesium ions in vermiculite clay. *Chemistry Letters*, **41**, 380–382.

Komy Z.R., Shaker A.M., Heggy S.E.M. & El-Sayed M.E.A. (2014) Kinetic study for copper adsorption onto soil minerals in the absence and presence of humic acid. *Chemosphere*, **99**, 117–124.

Matsumoto K. (2002) Decomposition methods of sparingly soluble materials. *BUNSEKI*, **2**, 60–66 (in Japanese).

McKinley J.P., Zachara J.M., Heald S.M., Dohnalkova A., Newville M.G. & Sutton S.R. (2004) Microscale distribution of cesium sorbed to biotite and muscovite. *Environmental Science & Technology*, **38**, 1017–1023.

Michael E.E. (2004) *Soil and Water Chemistry: An Integrative Approach*. CRC Press, Boca Raton, FL, USA.

Mimura H. & Kanno T. (1985) Distribution and fixation of cesium and strontium in zeolite A and chabazite. *Journal of Nuclear Science and Technology*, **22**, 284–291.

Mishra S., Sahoo S.K., Bossew P., Sorimachi A. & Tokonami S. (2018) Reprint of 'Vertical migration of radio-caesium derived from the Fukushima Dai-ichi Nuclear Power Plant accident in undisturbed soils of grassland and forest'. *Journal of Geochemical Exploration*, **184B**, 271–295.

Miura T., Takizawa N., Togashi K., Sasaki A. & Endo M. (2018) Adsorption/desorption characteristics of cesium ions on natural and synthetic minerals. *Journal of Ion Exchange*, **29**, 9–15.

Mukai H., Hirose A., Motai S., Kikuchi R., Tanoi K., Nakanishi T., Yaita T. & Kogure T. (2016) Caesium adsorption/desorption behavior of clay minerals considering actual contamination conditions in Fukushima. *Scientific Reports*, **6**, 21543.

Murota K., Saito T. & Tanaka S. (2016) Desorption kinetics of cesium from Fukushima soils. *Journal of Environmental Radioactive*, **153**, 134–140.

Nakao A., Ogasawara S., Sano O., Ito T. & Yanai J. (2014) Radiocesium sorption in relation to clay mineralogy of paddy soils in Fukushima, Japan. *Science of the Total Environment*, **468**, 523–529.

Onikata M., Kondo M., Hayashi N. & Yamanaka S. (1999) Complex formation of cation-exchanged montmorillonites with propylene carbonate: osmotic swelling in aqueous electrolyte solutions. *Clays and Clay Minerals*, **47**, 672–677.

Onodera M., Kirishima A., Nagao S., Takamiya K., Ohtsuki T., Akiyama D. & Sato N. (2017) Desorption of radioactive cesium by seawater from the suspended particle in river water. *Chemosphere*, **185**, 806–815.

Parajuli D., Takahashi A., Tanaka H., Sato M., Fukuda S., Kamimura R. & Kawamoto T. (2015) Variation in


https://doi.org/10.1180/clm.2018.35 Published online by Cambridge University Press

available cesium concentration with parameters during temperature induced extraction of cesium from soil. *Journal of Environmental Radioactivity*, **140**, 78–83.

Peeterbroeck S., Alexandre M., Jérôme R. & Dubois Ph. (2005) Poly (ethylene-*co*-vinyl cetate) /clay nanocomposites: effect of clay nature and organic modifiers on morphology, mechanical and thermal properties. *Polymer Degradation and Stability*, **90**, 288–294.

Royer B., Cardoso N.F., Lima E.C., Macedo T.R. & Airoldi C. (2010) A useful organofunctionalized layered silicate for textile dye removal. *Journal of Hazardous Materials*, **181**, 366–374.

Sawhney B.L. (1972) Selective sorption and fixation of cations by clay minerals: a review. *Clays and Clay Minerals*, **20**, 93–100.

Stagnaro S.Y.M., Rueda M.L., Volzone C. & Ortiga J. (2012) Structural modification lamellar solid by thermal treatment. Effect on the Cd and Pb adsorptions from aqueous solution. *Procedia Materials Science*, **1**, 180–184.

Staunton S. & Roubaud M. (1997) Adsorption of $^{137}Cs$ on montmorillonite and illite: effect of charge compensating cation, ionic strength, concentration of Cs, K, and fluvic acid. *Clays and Clay Minerals*, **45**, 251–260.

Tamura K., Sato H. & Yamagishi A. (2015) Desorption of $Cs^{+}$ ions from a vermiculite by exchanging with $Mg^{2+}$ ions: effects of $Cs^{+}$-capturing ligand. *Journal of Radioanalytical and Nuclear Chemistry*, **303**, 2205–2210.

Wu J., Li B., Liao J., Feng Y., Zhang D., Zhao J., Wen W., Yang Y. & Liu N. (2009) Behavior and analysis of cesium adsorption on montmorillonite mineral. *Journal of Environmental Radioactivity*, **100**, 914–920.

Zachara J.M., Smith S.C., Liu C., McKinley J.P., Serne R. J. & Gassman P.L. (2002) Sorption of $Cs^{+}$ to micaceous subsurface sediments from the Hanford site, USA. *Geochemica et Cosmochimica Acta*, **66**, 193–211.

Zaunbrecher L.K., Cygan R.T. & Elliott W.C. (2015) Molecular models of cesium and rubidium adsorption on weathered micaceous minerals. *The Journal of Physical Chemistry A*, **119**, 5691–5700.

https://doi.org/10.1180/clm.2018.35 Published online by Cambridge University Press